Electromagnetic Energy Harvesting from Flow Induced Vibration

D.-A. Wang, K.-H. Chang

Institute of Precision Engineering, National Chung Hsing University, Taichung 402, Taiwan, ROC

April 1, 2010

Abstract

A new electromagnetic energy harvester for harnessing energy from flow induced vibration is developed. It converts flow energy into electrical energy by fluid flow and electromagnetic induction. A finite element model for estimation of the generated voltage of the energy harvester is developed. A prototype of the energy harvester is fabricated and tested. Experimental results show that an output voltage of 10.2 mV_{pp} is generated when the excitation pressure oscillates with an amplitude of 254 Pa and a frequency of about 30 Hz. The values of the generated voltage based on the finite element computations agree well with the experiments. By detecting the voltage drop across a matched load, the instantaneous power is determined as 0.4 μW under an excitation frequency of 30 Hz and a pressure amplitude of 254 Pa in the pressure chamber.

Keywords: Electromagnetic; Energy harvester; Flow induced vibration

---

[*] Corresponding author. Tel.:+886-4-22840531; fax:+886-4-22858362

E-mail address: daw@dragon.nchu.edu.tw (D.-A. Wang).

1. Introduction

In recent years a considerable effort was focused on the development of energy harvesters or micropower generators. By scavenging energy from the environment, miniature sensing/actuating devices can be self-powered in order to avoid the replacement of finite power sources. The development of microsystems located in harsh environment further demands for low power consumption and almost no maintenance requirement.

One approach to harvest energy is to convert mechanical energy of ambient vibration into electrical energy by electromagnetic induction. Electromagnetic harvesters have been proposed and investigated by many researchers, for example, see [1-13]. It may be possible to harvest the mechanical energy from the motion of fluid. Sanchez-Sanz et al. [14] accessed the feasibility of using the unsteady forces generated by the Kármán street around a micro-prism in the laminar flow regime for energy harvesting. Holmes et al. [15] reported an axial-flux electromagnetic generator which was integrated with an axial-flow microturbine to extract power from ambient gas flows. An output voltage of 1.19 V_{pp} was achieved at a rotation rate of 30,000 rpm of their turbine. Herrault et al. [16] presented a rotary electromagnetic generator to harvest the mechanical energy of an air-driven turbine. Allen and Smits [17] used a piezoelectric membrane placed behind the von Kármán vortex street formed behind a bluff body to harvest energy from fluid motion. Taylor et al. [18] developed an Eel structure of piezoelectric polymer to convert mechanical flow energy to electrical power. They have demonstrated a complete Eel system with a generation and storage system in a wave tank. Tang et al. [19] designed a flutter-mill to generate electricity by extracting energy from fluid flow. When flutter takes place, a flexible plate placed between two parallel magnetic panels generates an electric potential. These authors utilized the flow-induced vibrations of fluid-structure interaction system to extract energy from the surrounding fluid flow [20]. The eel structures of Allen and Smits [17], Taylor et al. [18] and Tang et al. [19] have the potential to generate power from milli-watts to many watts depending on system size and flow velocity, but a power-generating eel has not been demonstrated. The devices of Holmes et al. [15] and Herrault et al. [16] require elaborate techniques for fabrication of their stator-rotor subcomponents and high rotation speeds for efficient energy harvesting. A device with simpler structure design and ease of application may be needed to extract energy from fluid motion.

In this paper, we develop a new energy-harvesting device based on flow-induced vibration. As illustrated in Fig. 1, a flow channel with a flexible diaphragm is connected to a flow source. The pressure in the chamber causes the diaphragm to deflect in the upward direction. As the pressure increases to the maximum, the diaphragm reaches its highest position. When the pressure drops, the diaphragm moves downward. As the pressure decreases to the minimum, the diaphragm reaches its lowest position. Thus, by connecting the energy harvester to an ambient flow source, which is capable of providing the pressure variation in the pressure chamber, the oscillating movement of the diaphragm with an attached permanent magnet surrounded by a coil makes the energy harvesting possible. The focus of this paper is on the investigation of energy extraction from diaphragm vibration induced by a fluid flowing in a channel. In order to access the feasibility of the proposed energy harvester, finite element analyses are carried out to obtain the pressure distribution within the chamber, the deflection of the diaphragm and the output voltage of the coil. Fabrication of the energy harvester is described. Experimental setup to measure the pressure, deflection and output voltage of the device is reported. The experimental results are compared with the results of the analyses.

2. Design

2.1 Operational principle

Our design of the electromagnetic energy harvester is based on the vibration induced by liquid flow in channels. The variation of the liquid pressure in the channel drives a polyester (PE) diaphragm with an attached permanent magnet surrounded by a fixed coil into vibration. The vibration energy is converted to electrical energy by the Faraday's law of induction [7,21,22]. An electromagnetic energy harvester is shown in Fig. 2(a). Fig. 2(b) is an exploded view of the energy harvester. It consists of a flow channel with two copper tubes, a PE diaphragm bonded to the channel, and a permanent magnet glued to the PE diaphragm. The permanent magnet is surrounded by a conducting coil which is guided around an inner housing. The inner housing of the coil is fixed by an outer housing.

This harvesting of flow energy via a flow-induced vibration is related to the response of a flexible diaphragm to an internal flow. The flow is bounded by the flexible structure and rigid walls. If the diaphragm has small inertia and is flexible enough to be able to respond rapidly to the fluctuating pressure field set up by the flow, one may expect that the diaphragm may oscillate with a frequency similar to that observed in the flow. When the fluctuating pressure is applied on the surface of the diaphragm, the diaphragm oscillates up and down, which causes the permanent magnet to vibrate at a frequency about the same as that of the pressure in the pressure chamber. The relative movement of the magnet to the coil results in a varying amount of magnetic flux cutting through the coil. According to the Faraday's law of induction, a voltage is induced in the loop of the coil. For convenience of analysis, finite element models are developed to estimate the pressure in the pressure chamber, the deflection of the PE diaphragm, and the voltage generated in the coil.

2.2 Finite element models

In order to analyze the deflection of the PE diaphragm and the voltage generated in the coil, pressure distribution within the chamber is obtained by finite element analysis. Three-dimensional flow analyses are carried out using a commercial software Fluent. In the analysis, a uniform velocity profile at the inlet along the direction of the inlet flow is applied. No-slip (zero velocity) conditions all along the channel walls are specified. The fluid is considered incompressible. A gage pressure 518 Pa is applied at the outlet of the channel due to the couplings with the copper tube. The Reynolds number is calculated in order to determine if the analysis is in the turbulent region. The Reynolds number of the flow channel can be determined by

$$\mathrm{Re} = \rho V D_h / \mu \tag{1}$$

where V is the flow velocity at the inlet of the diffuser element of the device, and μ is the dynamic viscosity of the water, 1.002×10^{-3} Pa $\cdot$ sec. D_h is the hydraulic diameter.

The liquid pressure in the chamber drives the PE diaphragm with the attached permanent magnet into vibration. Due to the symmetry of the geometry and the loading, the deflection of the diaphragm is analyzed by an axisymmetric model of the diaphragm and the attached magnet. Fig. 3(a) shows an axisymmetric slice of the diaphragm with a radius of 20 mm and a thickness of 100 μm, and the magnet with a radius of 5 mm and a thickness of 10 mm. A cylindrical coordinate system is also shown in the figure. The displacement in the r direction at $r = 0$ along the line $z = 0$ is constrained to represent the symmetry condition. The displacements in the r and z directions at $r = 20$ mm are constrained to represent the clamped boundary condition. A pressure, p, from $r = 0$ to $r = 20$ mm is applied in the $+z$ direction.

In this investigation, the diaphragm and the magnet are assumed to be linear elastic isotropic materials. The Young's modulus, the Poisson's ratio, and the density of the PE diaphragm are taken as 2.5 GPa, 0.25, and 1300 kg/m^3, respectively. The Young's modulus, the Poisson's ratio, and the density of the NdFeB magnet are taken as 41.4 GPa, 0.28, and 8100 kg/m^3, respectively. The commercial finite element program ABAQUS is employed to perform the computations. The first-order element, CAX4IH, is used for the vibration analyses under the pressure loading. The model is mainly for initial design and analysis of the vibration amplitude of the diaphragm under oscillating pressure loadings. Damping effects are neglected in the model.

In order to compute the output voltage of the proposed energy harvester and to examine its feasibility, two-dimensional axisymmetric finite element analyses are carried out. The dimensions of the energy harvester are indicated in Fig. 2. Due to the symmetry of the geometry and the loading, an axisymmetric model is considered. Fig. 3(b) shows an axisymmetric model of the magnet and the coil. A cylindrical coordinate system is shown in the figure. The dimensions of the magnet are indicated in the figure. The distance of the bottom surface of the magnet from the bottom of the coil is represented by

d. The material of background region indicated by the dashed rectangle is assigned to be air with a relative permeability of 1. The coil with 400 turns is model as strands in a rectangle made up of many individual insulated turns. A uniform current density is assumed throughout the rectangle. The magnetic vector potential is assumed to be zero at infinity, which suggests the model is isolated from other sources of magnetic fields. The magnet is made of Nd-Fe-B with a remanent flux density of 1.22 Tesla and a coercive field intensity of 927 kA/m.

Ansoft's Maxwell 2D magnetostatic field simulator is utilized to compute the static magnetic field arising from the magnet. Fig. 4(a) is a mesh of the axisymmetric model of the magnet and coil. The magnet is moved in the z direction based on a given history of the magnet displacement in order to calculate the rate of change of the flux ϕ. The induced voltage V in the coil is given by the Faraday's law of induction

$$V = \frac{d\phi}{dt} \tag{2}$$

In the analyses, the displacement history of the magnet is taken as the deflection history of the diaphragm by assuming a rigid connection between the magnet and the diaphragm. The simplified static model presented here is mainly for initial design and analysis of the voltage generated by the energy harvester. Magnetic losses are neglected in the model [23,24]. It is intended for quick evaluation of the effects of the device geometry, structure dimensions and material properties on the device performance. Here, we focus on the static analysis of the energy harvester for its potential applications in low-frequency environment.

2.3 Analyses

With the excitation frequency of 30 Hz, the experimental maximum and average values of flow velocity at the inlet, V, are 74 and 52 cm/sec, respectively, and the calculated Re are nearly 2467 and 1733, respectively. The pressure distributions of the flow channel at the maximum and average values of flow velocity at the inlet are obtained based on the laminar model of Fluent. The deviation of the pressure in the chamber along the symmetry axis are less than 0.2% for both cases, which is quite uniform. The maximum and the mean pressures at the center of the PE diaphragm are 805 Pa and 668 Pa at the maximum and average flow velocity at the inlet, respectively.

The peak and average value of the deflection of the diaphragm under the pressure loading with a mean pressure of 668 Pa and an amplitude of 137 Pa are 425 μm and 355 μm, respectively, based on the axisymmetric finite element analyses. The deflections of the diaphragm with the attached magnet under the pressure loadings may be large enough to provide the voltage output of the energy harvester. The dynamic analyses of the vibration of the diaphragm under the pressure loadings are intended for quick evaluation of the effects of the structure dimensions and material properties on the device performance. The simulated peak and average value of the deflection of the diaphragm agree with the experimental results, which are 443 μm and 358 μm, respectively. Note that the experimental inlet velocities of the flow channel are the input of the Flent analyses, and the simulated pressures of the Fluent analyses are the input of the deflection analyses based on the Abaqus computations.

In order to predict the output voltage of the energy harvester, finite element analyses are carried out based on an experimental deflection history of the PE diaphragm as shown in Fig. 5(a). The value of the distance d is taken as 58 μm, which is obtained by subtracting the initial distance between the bottom of the magnet and the bottom of the coil, 300 μm, from the mean of the deflection of the magnet, 358 μm, since the initial position of the bottom of the magnet is 300 μm lower than that of the bottom of the fixed coil. Fig. 4(b) shows the distribution of the magnetic flux lines for d = 58 μm. Fig. 5(b) shows the magnetic flux history cutting through the coil using Ansoft's Maxewell 2D software. Fig. 5(c) shows the induced voltage history in the coil using Eq. (2). The voltage oscillates with an amplitude of nearly 11 mV. The static analysis for the energy harvester can be used for low frequency applications. The simplified model for estimation of the voltage generated in the coil is only used for the feasibility study of the proposed energy harvesting device.

3. Fabrication, experiments and discussions

3.1 Fabrication

In order to verify the effectiveness of the proposed energy harvesting device, a prototype of the energy harvester is fabricated. Fig. 6 shows the fabrication steps. First, a flow channel is carved from a block of acrylic by a milling machine (PNC-3100, Roland DGA Co., Japan). Next, the inlet and outlet of the flow channel are prepared by drilling holes in the front and back ends of the flow channel block. Subsequently, a PE diaphragm of 100 μm in thickness is glued to the flow channel by an epoxy adhesive (3M, DP460) cured at a temperature of $60^{\circ}C$ for 3 hours. Two copper tubes are fastened into the inlet and outlet hole, respectively. Next, the magnet is glued to the PE diaphragm. Finally, the inner housing with the coil wrapped around its exterior surface is placed inside the outer housing, which is then glued to the top surface of the flow channel block to complete the assembly steps. The initial distance between the top surface of the PE diaphragm and the bottom of the coil is 300 μm. Fig. 7(a) and (b) are photos of the flow channel with the magnet glued to it and an assembled energy harvester, respectively.

4.2 Experiments

Fig. 8 is a schematic of the experimental apparatus for testing of the fabricated device. The energy harvester is placed on a platform of a tank. Tap water is pumped into the inlet of the energy harvester through a pulse pump to provide a periodic pressure in the pressure chamber of the energy harvester. The oscillating deflection of the PE diaphragm is measured by a Philtec D6 fiberoptic displacement sensor. The induced voltage of the coil is filtered by a Stanford SR560 preamplifier and is recorded and analyzed by a data acquisition unit (PCI-5114, National Instruments Co., US). Fig. 9 is a photo of a close-up view of the experimental apparatus. The experimental results are shown in Fig. 10. Fig. 10(a) shows the pressure history in the pressure chamber, where the mean pressure and the pressure difference $P_{max} - P_{min}$ within the pressure chamber is 684 and 508 Pa, respectively. The pressure is measured with a subminiature pressure sensor (PS-05KC, Kyowa Electronic Instruments Co. Ltd., Japan) embedded in the pressure chamber. The pressure sensor is connected to a data acquisition unit (DBU-120A, Kyowa Electronic Instruments Co. Ltd., Japan). The measured deflection history of the PE diaphragm is shown in Fig. 10(b). The diaphragm is oscillated about a deflected position of 358 μm with an amplitude of nearly 85 μm. The output voltage of the coil is shown in Fig. 10(c). The output peak-to-peak voltage for an oscillation amplitude of 254 Pa and an excitation frequency of 30 Hz of the pressure in the pressure chamber is nearly 10 mV. The experimental results do not show transient responses since they are recorded at steady state vibration.

The measured voltages generated by several values of the pressure difference in the pressure chamber are shown in Fig. 11. The simulation results are also shown in the figure. The output voltages based on the model and the experiment increase nearly linearly with the pressure difference in the pressure chamber. The slope of the nearly linear curve of the simulated data is close to that of the experimental data. This indicates that the model provides a relatively accurate prediction of the induced voltage of the coil. The output voltages of the experiments are slightly lower than those based on the model. This might be due to the magnetic losses neglected in the model and the misalignment during the assembly process of the device. The model can be effective as a design tool to determine the size and excitation pressure level necessary to provide the desired voltage generation.

In order to evaluate the harvesting system, experiments on the electrical power output of the device are performed. The internal electrical resistance of the device is measured by a LCR meter (WK 4235, Wayne Kerr Electronics, Ltd., UK). A matched load of 25 Ω to maximize output power is connected to the device. By detecting the voltage drop across the matched load, the instantaneous power is determined as 0.4 μW under an excitation frequency of 30 Hz and a pressure amplitude of 254 Pa in the pressure chamber.

In this investigation, the device is operated at its first resonance frequency. The measured resonance frequency of the device is 30 Hz, which is the excitation frequency used throughout the investigation. Most resonance-based energy harvesting devices have focused on single-frequency ambient energy [25]. When the ambient excitation is at a single frequency, the design of the energy harvesting device can be tailored to the ambient frequency available. For random and broadband ambient flow sources, the device may not be robust. To account for the variations in the excitation frequency, a device with an array of structures with various resonance frequencies can be utilized [26]. The other possible route to account for the random ambient flow sources is to minimize the mechanical damping or maximize the electromechanical coupling of the device [25]. A structure with multiple resonant frequencies may also be considered for energy harvesting from random vibrations with multiple resonant peaks, for example a segmented composite beam with embedded piezoelectric layers [27].

In order to generate the pressure fluctuation in the channel, a pulse pump is used to pump tap water into the flow channel in the laboratory environment. Energy can be harvested from unsteady geophysical flows (ocean or river currents). The developed model for estimation of the generated voltage, which is verified by the experiments carried out in this investigation, can be used for quick estimation of the design parameters on the performance of the energy harvester.

Compared to other researchers' work to extract energy from flow-induced vibrations of fluid-structure interaction system, the presented design might be simpler in its structure and fabrication, since the devices of Holmes et al. [15] and Herrault et al. [16] consist of stator-rotor subcomponents, which need elaborate fabrication steps, and a high rotation speed may be needed for efficient energy harvesting. The eel structure of Allen and Smits [17] has proved to be feasible by simulation and hydrodynamic testing, but a power-generating eel is not demonstrated. Taylor et al. [18] have demonstrated an eel structure with a power generation and storage system in a wave tank. The length, width and thickness of their eel are 9.5", 3", and 0.15 mm, respectively. The challenge to design and deploy a miniaturized eel-like system remains. Although the output power of our device is relatively low, given the structure design of the flow channel and the piezoelectric film, the dimensions of the device can be decreased for construction of a miniaturized system to harvest energy from flow motion by solid-fluid interaction.

4. Conclusions

An electromagnetic energy harvester is developed. The energy is harvested from flow induced vibration. The pressure oscillation in the pressure chamber of the harvester results in a periodical deflection of the PE diaphragm and therefore the voltage induction in the coil surrounding a permanent magnet which is glued to the PE diaphragm. Finite element models of the device are developed for quick evaluation of effects of device dimensions, pressure loads and material properties on the performance of the energy harvester. A prototype of the energy harvester is fabricated and tested. The measurements conducted in various pressure differences in the pressure chamber of the device show that the maximum output voltage is approximately 11 mV_{pp}, when the excitation pressure oscillates with an amplitude of 254 Pa and a frequency of about 30 Hz. The solutions of the generated voltage based on the finite element computations agree well with the experiments. By detecting the voltage drop across a matched load, the instantaneous power is determined as 0.4 μW under an excitation frequency of 30 Hz and a pressure amplitude of 254 Pa in the pressure chamber.

Sources of flow induced vibration can be unsteady geophysical flows (ocean or river currents). The periodic vortex shedding behind a blunt body immersed in a steady stream causes a pressure oscillation in the stream. This regular, periodic shedding can be integrated into the flow channel of the proposed device to scavenge the flow energy.

Acknowledgement

This work was financially supported by Precision Machinery Research and Development Center (Contract Number: 98TR10). Partial support of this work by a grant from National Science Council, Taiwan (Grant Number: NSC 96-2221-E-005-095) is greatly appreciated. The authors would like to express their appreciation to the National Center for High-Performance Computing (NCHC), Taiwan for their assistance. Helpful discussions with Professor Yuen-Wuu Suen of National Chung Hsing University, Taiwan, R.O.C. are greatly appreciated.

References

[1] C.B. Williams, R.B. Yates, Analysis of a micro-electric generator for microsystems, Sensors and Actuators A 52 (1996) 8-11.

[2] N.N.H. Ching, H.Y. Wong, W.J. Li, P.H.W. Leong, Z. Wen, A laser-micromachined multi-modal resonating power transducer for wireless sensing systems, Sensors and Actuators A 97-98 (2002) 685-690.

[3] P. Glynne-Jones, M.J. Tudor, S.P. Beeby, N.M. White, An electromagnetic, vibration-powered generator for intelligent sensor systems, Sensors and Actuators A 110 (2004) 344-349.

[4] P.-H. Wang, X.-H. Dai, D.-M. Fang, X.-L. Zhao, Design, fabrication and performance of a new vibration-based electromagnetic micro power generator, Microelectronics Journal 38 (2007) 1175-1180.

[5] S. Cheng, N. Wang, D.P. Arnold, Modeling of magnetic vibrational energy harvesters using equivalent circuit representations, Journal of Micromechanics and Microengineering 17 (2007) 2328-2335.

[6] T. von Büren, G. Tröster, Design and optimization of a linear vibration-driven electromagnetic micro-power generator, Sensors and Actuators A 135 (2007) 765-775.

[7] I. Sari, T. Balkan, H. Kulah, An electromagnetic micro power generator for wideband environmental vibrations, Sensors and Actuators A 145-146 (2008) 405-413.

[8] D. Spreemann, D. Hoffmann, B. Folkmer, Y. Manoli, Numerical optimization approach for resonant electromagnetic vibration transducer designed for random vibration, Journal of Micromechanics and Microengineering 18 (2008) 104001.

[9] C.R. Saha, T. O'Donnell, N. Wang, P. McCloskey, Electromagnetic generator for harvesting energy from human motion, Sensors and Actuators A 147 (2008) 248-253.

[10] S. Kulkarni, E. Koukharenko, R. Torah, J. Tudor, S. Beeby, T. O'Donnell, S. Roy, Design, fabrication and test of integrated micro-scale vibration-based electromagnetic generator, Sensors and Actuators A 145-146 (2008) 336-342.

[11] C. Serre, A. Pérez-Rodríguez, N. Fondevilla, E. Martincic, J.R. Morante, J. Montserrat, J. Esteve, Linear and non-linear behavior of mechanical resonators for

optimized inertial electromagnetic microgenerators, Microsystem Technologies 15 (2009) 1217-1223.

[12] B. Yang, C. Lee, W. Xiang, J. Xie, J.H. He, R.K. Kotlanka, S.P. Low, H. Feng, Electromagnetic energy harvesting from vibrations of multiple frequencies, Journal of Micromechanics and Microengineering 19 (2009) 035001.

[13] B.P. Mann, N.D. Sims, Energy harvesting from the nonlinear oscillations of magnetic levitation, Journal of Sound and Vibration 319 (2009) 515-530.

[14] M. Sanchez-Sanz, B. Fernandez, A. Velazquez, Energy-harvesting microresonator based on the forces generated by the Karman street around a rectangular prism, Journal of Microelectromechanical Systems 18 (2009) 449-457.

[15] A.S. Holmes, G. Hong and K.P. Pullen, Axial-flux permanent magnet machines for micropower generation, Journal of Microelectromechanical Systems 14 (2005) 54-62.

[16] F. Herrault, D.P. Arnold, I. Zana, P. Galle, M.G. Allen, High temperature operation of multi-watt, axial-flux, permanent-magnet microgenerators, Sensors and Actuators A 148 (2008) 299-305.

[17] J.J. Allen, A.J. Smits, Energy harvesting eel, Journal of Fluid and Structures 15 (2001) 629-640.

[18] G.W. Taylor, J.R. Burns, S.M. Kammann, W.B. Powers, T.R. Welsh, The energy harvesting eel: A small subsurface ocean/river power generator, IEEE Journal of Oceanic Engineering 26 (2001) 539-547.

[19] L. Tang, M.P. Païdoussis, J. Jiang, Cantilevered flexible plates in axial flow: Energy transfer and the concept of flutter-mill, Journal of Sound and Vibration 326 (2009) 263-276.

[20] R.D. Blevins, Flow-induced vibration, 2nd edition, Van Nostrand Reinhold, New York, 1990.

[21] B.S. Lee, S.C. Lin, W.J. Wu, X.Y. Wang, P.Z. Chang, C.K. Lee, Piezoelectric MEMS generators fabricated with an aerosol deposition PZT thin film, Journal of Micromechanics and Microengineering 19 (2009) 065014.

[22] E. M. Purcell, *Electricity and magnetism*, 2nd edition, McGraw-Hill, Boston, US, 2004.

[23] G. Bertotti, General properties of power losses in soft ferromagnetic materials, IEEE Transactions on Magnetics 24 (1988) 621-630.

[24] G. Poulin, E. Sarraute, F. Costa, Generation of electrical energy for portable devices Comparative study of an electromagnetic and a piezoelectric system, Sensors and Actuators A 116 (2004) 461-471.

[25] S. Adhikari, M. I. Friswell and D. J. Inman, Piezoelectric energy harvesting from broadband random vibrations, Smart Materials and Structures, 18 (2009) 115005.

[26] J.-Q. Liu, H.-B. Fang, Z.-Y. Xu, X.-H. Mao, X.-C. Shen, D. Chen, H. Liao and B.-C. Cai, A MEMS-based piezoelectric power generator array for vibration energy harvesting, Microelectronics Journal, 39 (2008) 802-806.

[27] S. Lee, B. D. Youn and B. C. Jung, Robust segment-type energy harvester and its application to a wireless sensor, Smart Materials and Structures, 18 (2009) 095021.

Biography

Dung-An Wang received the Ph.D. degree in mechanical engineering from the University of Michigan at Ann Arbor, in 2004. He is currently an Assistant Professor in the Institute of Precision Engineering, National Chung Hsing University, Taiwan, ROC. His research interests include micromachined resonators and actuators, piezoelectric actuators, microassembly and compliant mechanisms.

Kai-Hun Chang received the B.S. degree in mechanical engineering from the Chinese Culture University, Taiwan, ROC, in 2007, and is currently working towards the M.S. degree in the Institute of Precision Engineering, National Chung Hsing University, Taiwan, ROC. His research interests are electromagnetic actuators, and microassembly.

List of figures

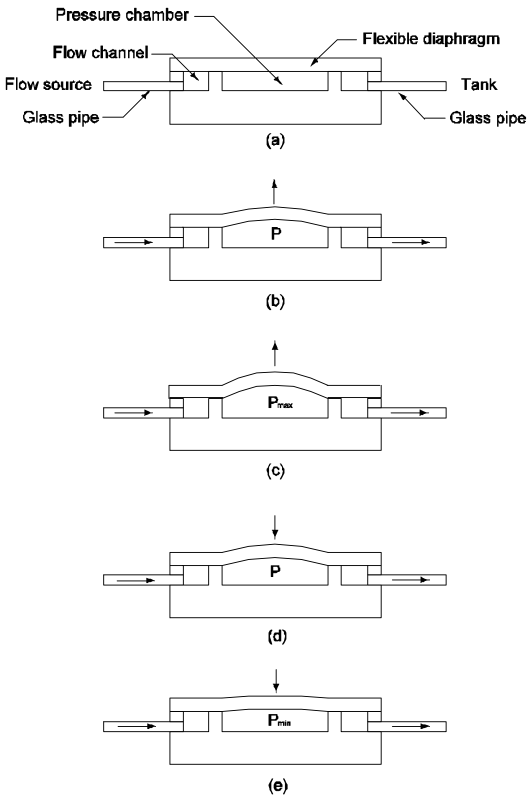

Fig. 1. Operation of an electromagnetic energy harvester.

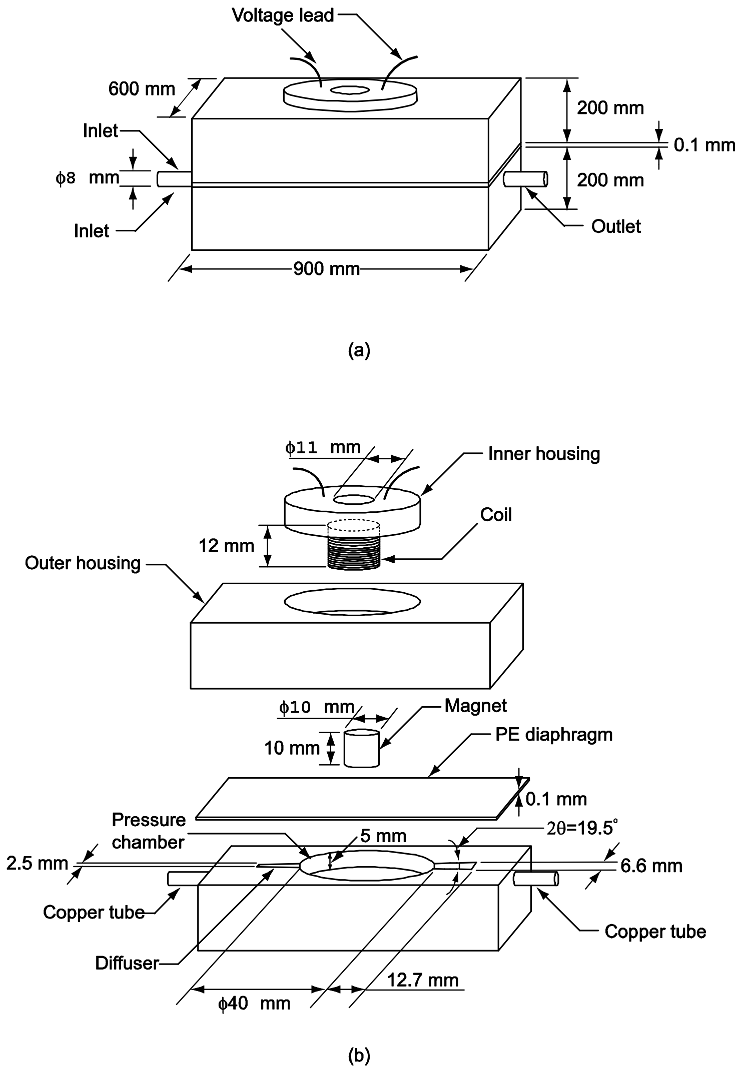

Fig. 2. (a) An assembled energy harvester. (b) Components of the energy harvester.

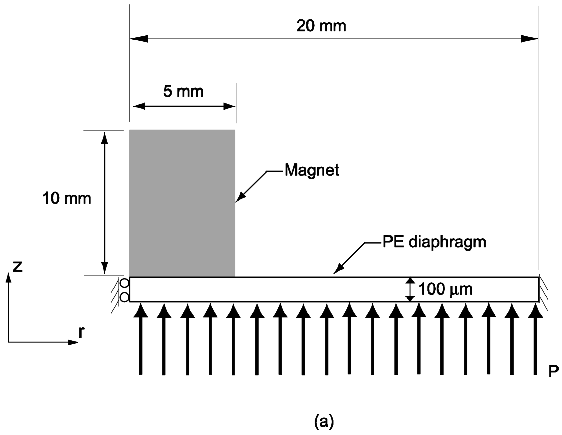

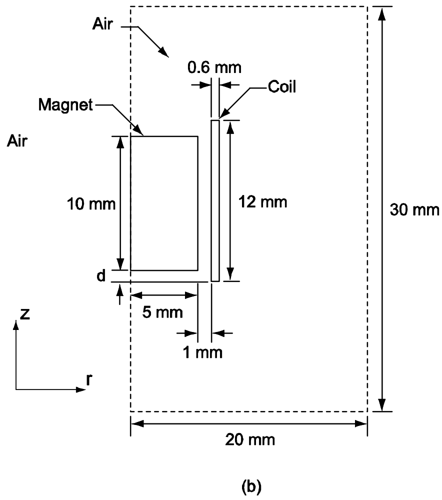

Fig. 3. (a) An axisymmetric model of the diaphragm and the magnet. (b) An axisymmetric model of the magnet and coil.

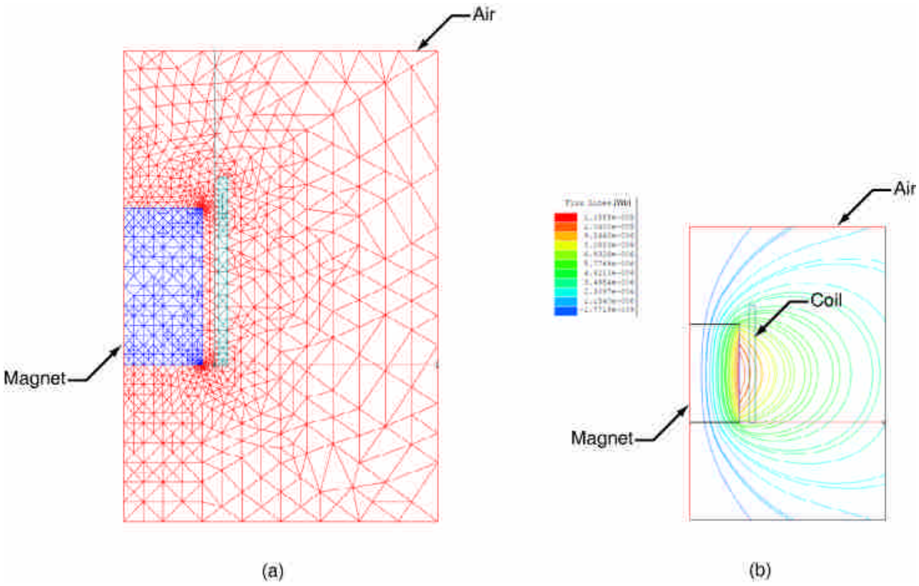

Fig. 4. (a) A mesh of an axisymmetric model of the magnet and coil. (b) Magnetic flux lines along which the magnetic flux density is directed.

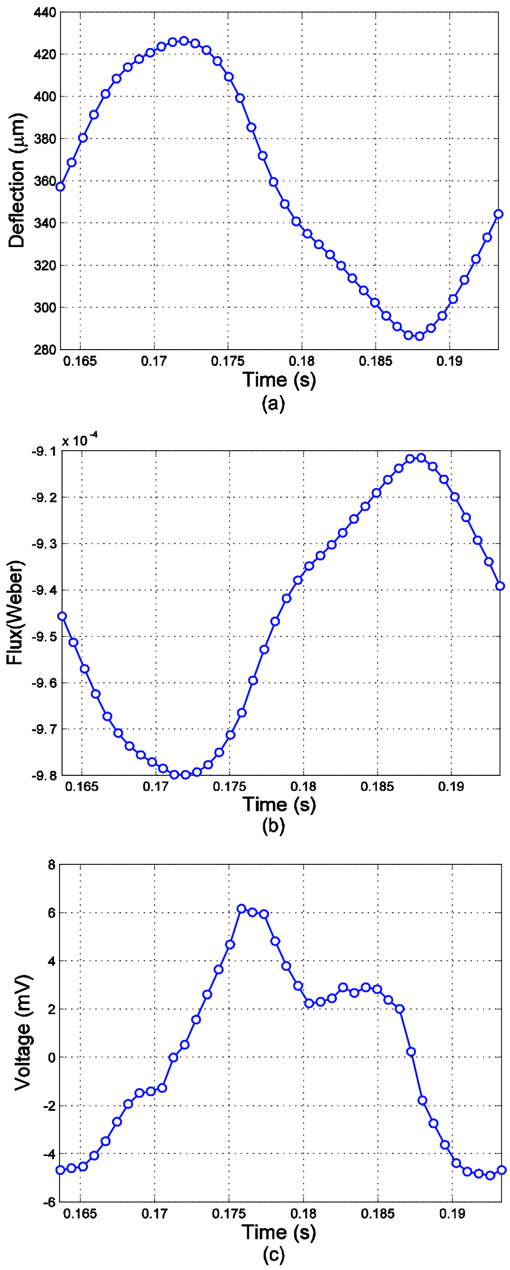

Fig. 5. (a) A typical deflection history of the PE diaphragm. (b) History of magnetic flux cutting through the coil. (c) Output peak-to-peak voltage history.

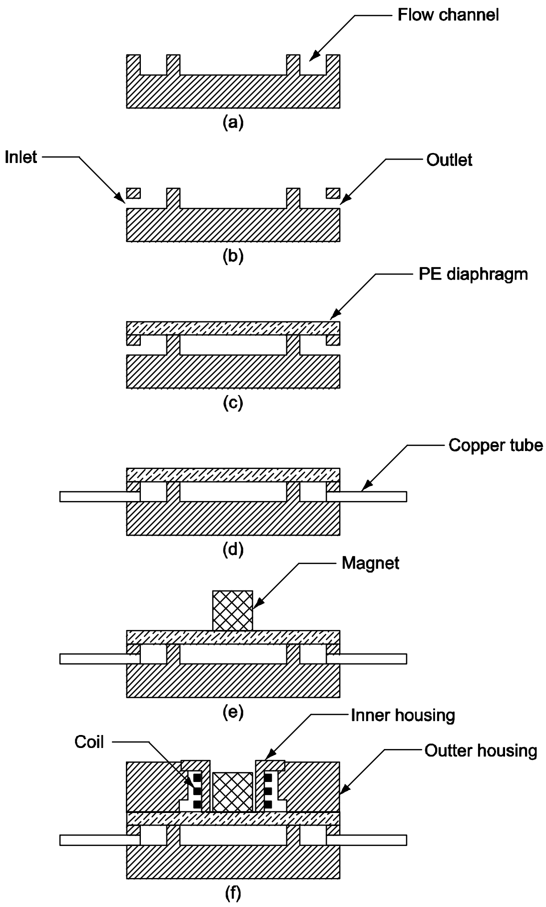

Fig. 6. Assembly steps of the energy harvester.

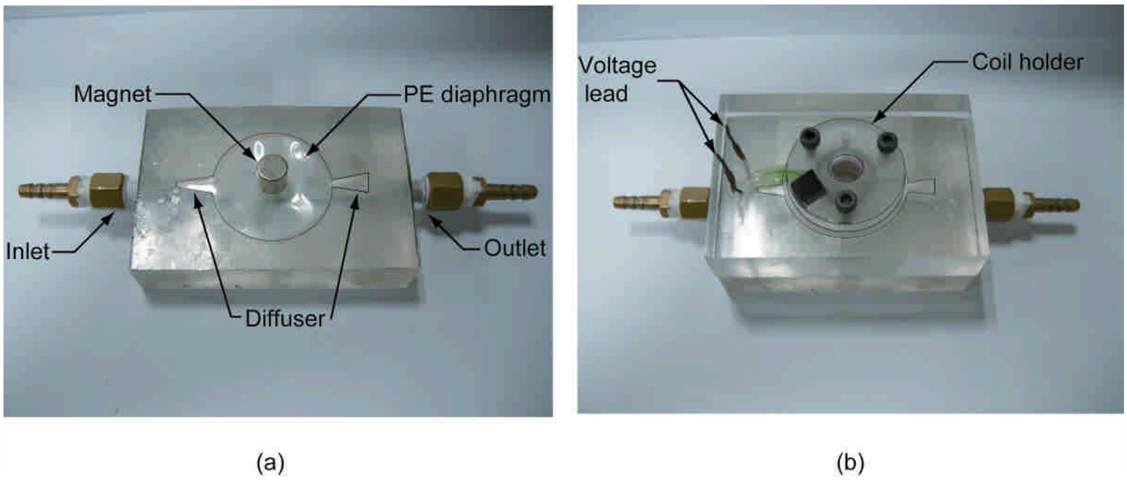

Fig. 7. (a) Flow channel with the magnet glued to it. (b) Assembled energy harvester.

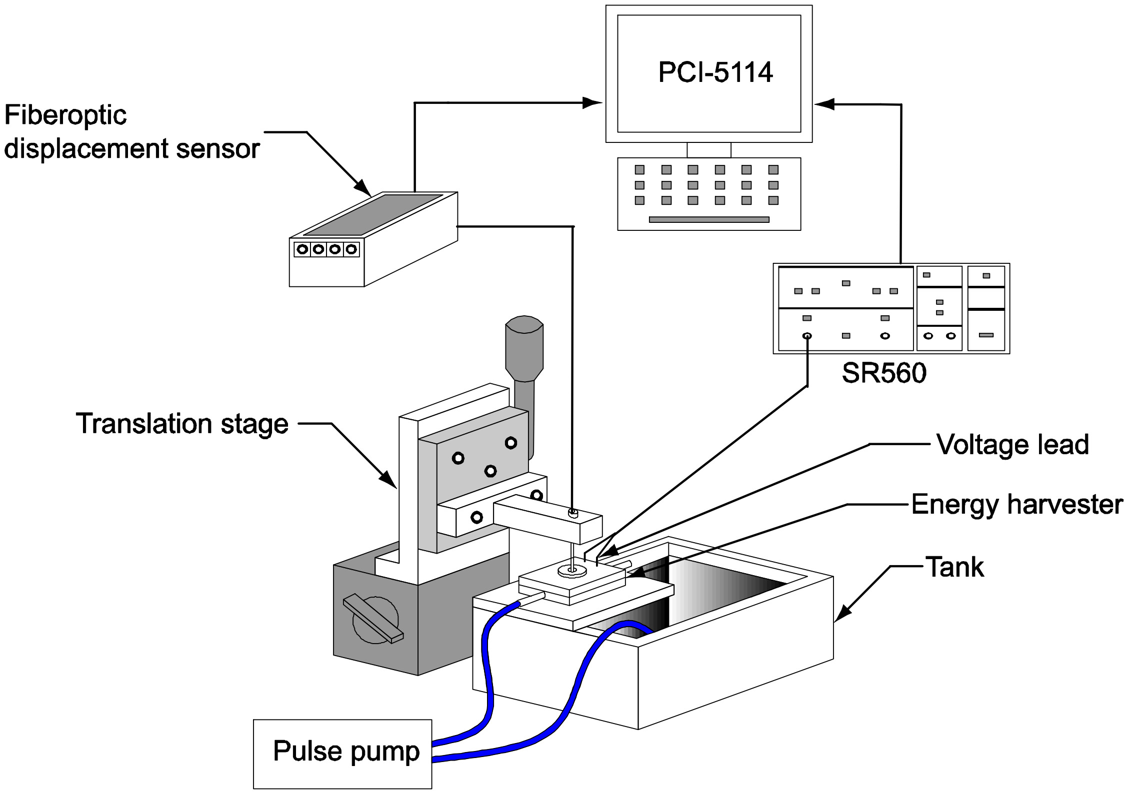

Fig. 8. Schematic of the experimental apparatus.

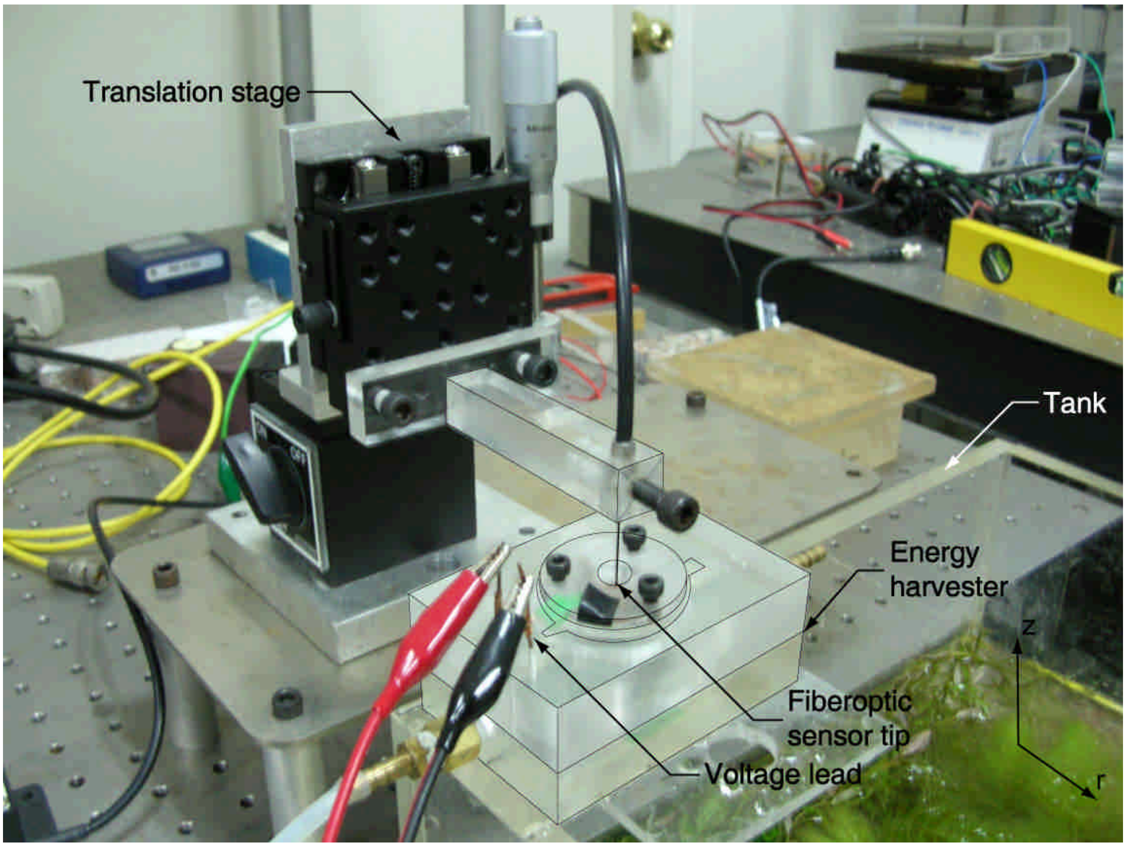

Fig. 9. Close-up view of the experimental apparatus.

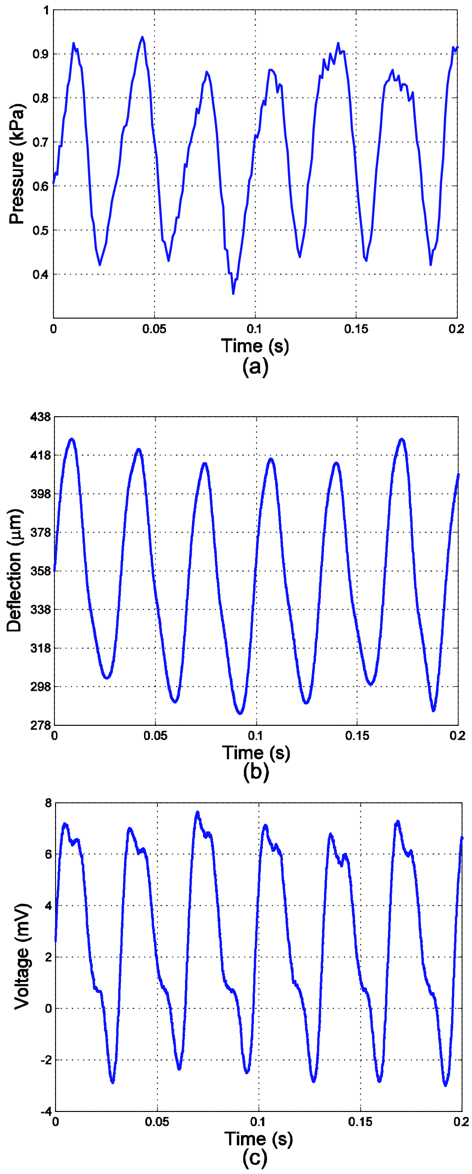

Fig. 10. Experimental results. (a) Pressure history in the pressure chamber. (b) Deflection history of the center of the PE diaphragm. (c) Output voltage history.

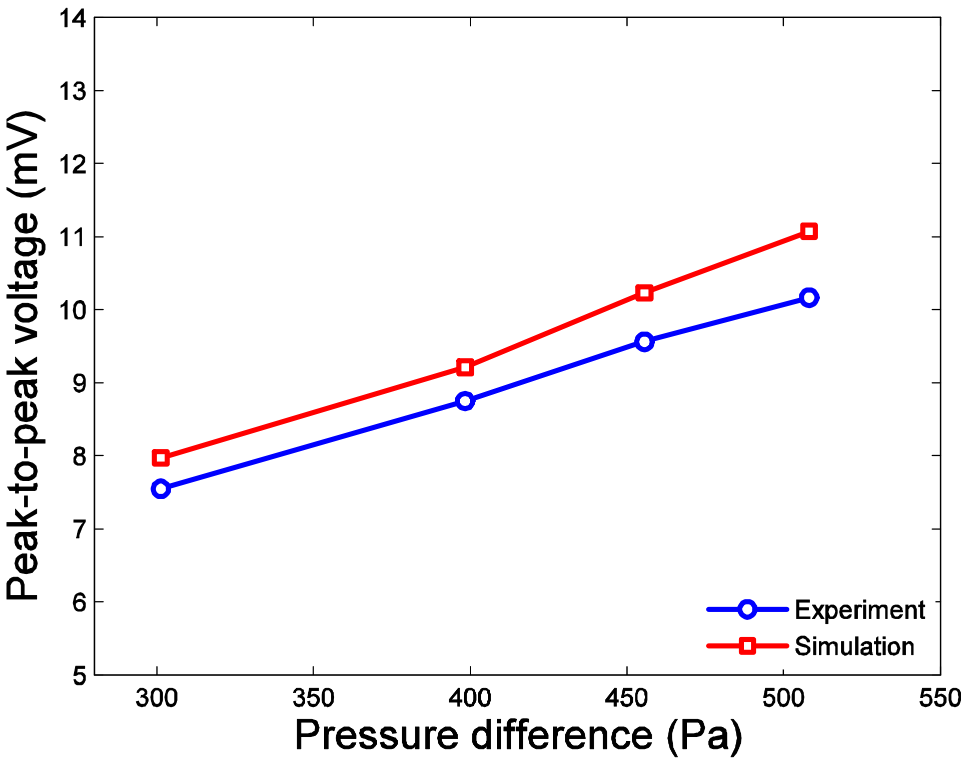

Fig. 11. Output voltage as a function of the pressure difference in the pressure chamber.